1P5-4

Basic examination for selecting probability distribution model in ultrasound tissue characterization

Shohei Mori[1†*], Mototaka Arakawa[2,1], Tadashi Yamaguchi[3], Hiroshi Kanai[1,2], and Hiroyuki Hachiya[4] ([1]Grad. School Eng., Tohoku Univ.; [2]Grad. School Biomed. Eng., Tohoku Univ.; [3]Center for Frontier Medical Engineering, Chiba Univ.; [4]Tokyo Tech)

1. Introduction

An analysis of echo envelope statistics contributes to a quantification of diseases such as liver fibrosis[1)] and fatty liver[2,3)]. In the statistic-based tissue characterization, the probability density function of the echo envelope amplitudes is fitted by a model function, and the tissue characteristics are quantified by model parameters. Therefore, using an appropriate model is essential for the correct tissue characterization. In the present study, we examined a method for selecting the probability distribution model which is appropriate for analyzing the obtained echo data.

2. Methods

2.1 Probability distribution models

The most basic probability distribution model is a Rayleigh (RA) distribution. When the scatterers with sufficiently smaller than the wavelength are randomly, densely, and homogeneously distributed, the echo envelope x follows the RA distribution.[4)]

$$p_{\mathrm{RA}}(x|\sigma_{\mathrm{RA}}) = \frac{2x}{\sigma_{\mathrm{RA}}^2}\exp\left(-\frac{x^2}{\sigma_{\mathrm{RA}}^2}\right), \qquad (1)$$

where σ_{RA} is a scale parameter.

The RA distribution is effective to evaluate the normal liver tissue. For the fibrotic liver, however, the multi-Rayleigh (MRA) distribution, which is a mixture model of multiple RA distributions with different scale parameters, is effective.[1)] For the evaluation of fatty liver, the Nakagami (NA)[2)] and double-NA[3)] distributions are effective.

2.2 Moment-based classification

To quantitatively select the appropriate probability distribution model, we examined a moment-based classification. The moment is a basic statistical property and given by

$$M_k = \mathrm{E}[x^k], \qquad (2)$$

where k is an order of the moment and $\mathrm{E}[\cdot]$ is an operation of the expectation.

As a result of the central limit theorem, the moment of random variables following a certain probability distribution model with fixed model parameters follows a normal distribution. Moreover, the expectation and standard deviation of the normal distribution are theoretically determined.[5)]

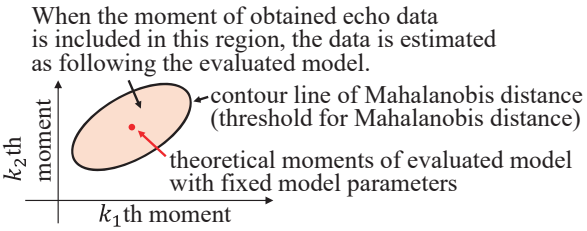

Fig. 1 Schematic of moment-based classification.

Based on this property, the deviation of the moment of the obtained echo data from that of a certain probability distribution model can be quantified using a Mahalanobis distance, which is a distance normalized by the covariance of the multidimensional normal distribution.[1)] As shown in **Fig. 1**, whether the obtained echo data follows the evaluated model is determined by the threshold processing to the Mahalanobis distance. As the squared Mahalanobis distance follows a chi-squared distribution, the threshold for the Mahalanobis distance can be quantitatively determined based on the cumulative chi-squared distribution.[1)]

In our previous study[1)], we used this Mahalanobis distance to estimate the number of tissue components in the fibrotic liver (*i.e.* number of RA components in the MRA distribution). In the present study, we applied this method to determine the appropriate probability distribution model.

For the obtained echo data, the parameters of NA and MRA distributions were estimated by the maximum likelihood estimation method. Then, the squared Mahalanobis distances of moments of obtained echo data from that of RA (normal liver condition), NA (fatty liver condition), and MRA (fibrotic liver condition) distributions with estimated parameters, respectively, were evaluated. Finally, whether the obtained echo data follows each distribution model was evaluated by the threshold processing to the squared Mahalanobis distance. The first, third, fourth, and fifth orders of moments were used for calculating the Mahalanobis distance.

2.3 Ultrasonic simulation

To simulate the NA condition, scattered density was set to 1 scatterer per the area of full width at half maximum (FWHM) of the ultrasound spatial resolution. The average of Nakagami m parameters, which is an indicator of the scattered density, estimated for the simulated ultrasound B-

E-mail: [†*]mori@tohoku.ac.jp

mode image was 0.72.

To simulate the RA and MRA conditions, two types of scatterer distributions with different reflection coefficients ($\sqrt{3}$ times difference) were placed adjacent to each other. The scattered density was set to 10 scatterers per FWHM of the ultrasound spatial resolution, for both scatterer distributions.

The radiofrequency (RF) echo signals were obtained from the scatterer distributions by Field II. [6,7] The transmitted and sampling frequencies were set to 7.5 and 40 MHz, respectively.

3. Results and Discussions

Figures 2(a) and 2(b) show the results for the simulation with NA condition and that with RA and MRA conditions, respectively. Figure 2(i) shows the simulated ultrasound B-mode images. Figures 2(ii-iv) show the regions estimated as following the RA, NA, or MRA distributions, respectively. The window shown in Fig. 2(a)(i) was scanned pixel by pixel and the squared Mahalanobis distance was evaluated for each window, independently.

As shown in Fig. 2(a)(ii), there were no regions that follow the RA distribution because the scattered density was low. On the other hand, the NA distribution, which can express the condition of low scattered density, could express the entire regions, as shown in Fig. 2(a)(iii). Although the MRA distribution is not a model for expressing the condition of low scattered density, there were many regions that the window data could be expressed by the MRA distribution, as shown in Fig. 2(a)(iv).

In Fig. 2(b), the MRA distribution could express the entire regions, as shown in Fig. 2(b)(iv), because the MRA distribution includes the RA distribution and can express the mixture of RA distributions. As expected, the RA distribution could express the regions of the single scatterer distribution (outer regions of red dashed lines) and could not express the mixture regions (inner regions of red dashed lines), as shown in Fig. 2(b)(ii).

The NA distribution could also express the regions of the single scatterer distribution, as shown in Fig. 2(b)(iii), because the NA distribution includes the RA distribution. However, although the NA distribution is not a model for the mixture of multiple scatterer distributions, there were regions that the window data set in the mixture region could be expressed by the NA distribution.

Thus, there were regions that the window data could be expressed by both NA and MRA distributions. These results indicate that other than the condition of the RA distribution, there are model parameters in the NA (fatty liver condition) and MRA (fibrotic liver condition) distributions that have statistically similar characteristics, which should be examined in detail in the future.

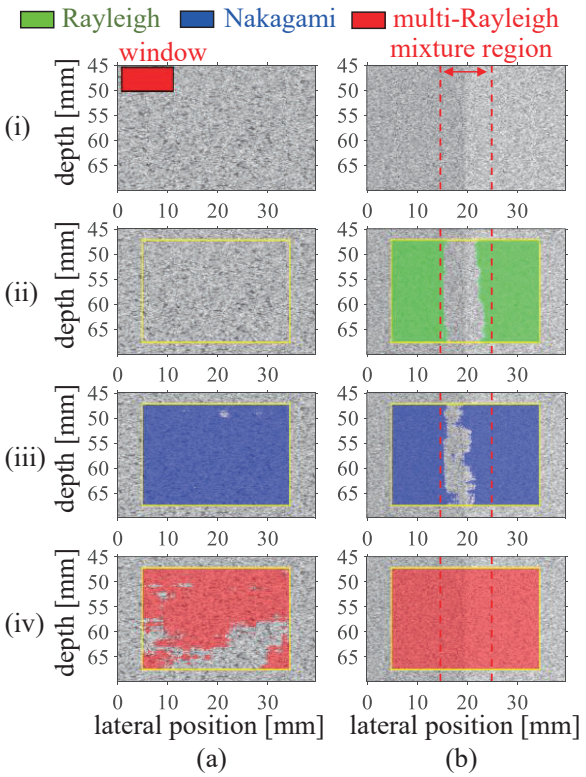

Fig. 2 (a) Low scattered density condition. (b) Mixture condition of two types of scatterer distributions with different reflection coefficients. (i) Ultrasound B-mode image. (ii-iv) Regions estimated as following (ii) Rayleigh, (iii) Nakagami, and (iv) multi-Rayleigh distributions.

4. Conclusion

Based on the moments, whether a certain probability distribution model can express the obtained echo data was evaluated. In the future, we will examine a method to distinguish between NA and MRA distributions for the echo data that can be expressed by both models.

Acknowledgment

This work was supported in part by JSPS KAKENHI 21K14166.

References

1) S. Mori, S. Hirata, T. Yamaguchi, et al., Jpn. J. Appl. Phys. **57**, 07LB07 (2018).
2) Z. Zhou, D.-I. Tai, Y.-L. Wan, et al., Ultrasound Med. Biol. **44**, 1327 (2018).
3) K. Tamura, J. Mamou, K. Yoshida, et al., Jpn. J. Appl. Phys. **59**, SKKE23 (2020).
4) C. B. Burckhardt, IEEE Trans. Sonics Ultrason. **25**, 1 (1978).
5) S. Mori, M. Arakawa, H. Kanai, et al., Jpn. J. Appl. Phys. **62**, SJ1045 (2023).
6) J. A. Jensen, Med. Biol. Eng. Comput. **34** [Suppl. 1, Part 1], 351 (1996).
7) J. A. Jensen and N. B. Svendsen, IEEE Trans. Ultrason. Ferroelectr. Freq. Control **39**, 262 (1992).